

Circularly Polarized Tunable Graphene-Patch over SiO₂ substrate for THz Applications

Nagesh Kallollu Narayaswamy

Nagarjuna College of Engineering and Technology

Manju Ramrao Bhosle

Government Engineering College

Krishna Kanth Varma Penmatsa

S.R.K.R. Engineering College

Ajay Kumar Dwivedi (✉ er.ajaydwivedi@gmail.com)

Nagarjuna College of Engineering and Technology

Research Article

Keywords: THz Antenna, Graphene, Circular Polarization, Biomedical Application

Posted Date: July 11th, 2022

DOI: <https://doi.org/10.21203/rs.3.rs-1752541/v2>

License: © ⓘ This work is licensed under a Creative Commons Attribution 4.0 International License.

[Read Full License](#)

Abstract

In this communication, a graphene-based radiator is designed and analyzed at THz frequency. A tilted dumbbell-shaped aperture is loaded on a graphene patch for creating degenerated orthogonal mode with 90° phase shift, which in turn produces circularly polarized (CP) waves. Graphene patch is placed over SiO_2 substrate. Slot loading in graphene patch shifts the frequency band due to a reduction in effective permittivity. Another important feature of the proposed antenna is to provide a tunable feature in the frequency response and axial ratio by changing the chemical potential. The proposed antenna operates from 5.85 THz to 6.05 THz. 3-dB axial ratio is obtained from 5.85 THz to 5.95 THz. Good value of gain, as well as left-handed circular polarization characteristics, makes the proposed THz antenna in biomedical applications

I. Introduction

The modern world of wireless communications moves towards the THz spectrum because it provides a higher data rate with wider impedance bandwidth [1]. The main challenge to designing an antenna at THz frequency is the metallic losses in the case of printed radiators and non-planarity in the dielectric resonators [2]. These challenges can be overcome by 2D materials such as graphene. It can also provide reconfigurability to the antenna characteristics by simply varying its chemical potential [3].

Polarization is one of the most important parameters in any radiator. A circularly polarized antenna makes the transmitter and receiver orientation independent and reduces the effect of multipath fading [4]. Very few research articles are available on circularly polarized THz antenna. Varshney et.al. proposed a ceramic-based nano-cylindrical ceramic antenna, which supports the CP waves from 188.5–199.6 THz. However, there is no tunable feature in this radiator [5]. Ullah et.al proposed a patch antenna loaded with an S-shaped slot. It works from 0.258 THz to 0.355 THz. But, its physical size is quite large $1200 \times 460 \times 127 \mu\text{m}^3$ [6]. Varshney et.al. proposed stair shaped slot-loaded graphene patch, which supports CP waves in dual-frequency bands i.e. 2.94–2.99 THz and 4.99–5.01 THz [7]. Shalini et.al. designed an E-shaped graphene patch, which supports approx. 0.05 THz axial ratio below 3-dB [8]. Gupta et.al. proposed a hybrid radiator i.e. combination of graphene and ceramic. It creates CP waves from 3.95 THz to 4.1 THz. Due to the presence of ceramic; the antenna structure becomes bulkier [9].

This article explains the design of a tunable tilted dumbbell-shaped aperture loaded graphene patch, which supports the circular polarization feature. This antenna operates from 5.85 THz to 6.05 THz. Change in chemical potential of graphene patch provides the tunable feature inside the radiator. The sense of polarization can easily be controlled by simply changing the orientation of the slot. For better understanding, the article is divided into sub-categories i.e. antenna design layout, antenna analysis, optimized antenna outcome, and conclusion.

Ii. Antenna Design Layout

The structural layout of the proposed graphene-based THz antenna is displayed in Fig. 1. A tilted dumbbell-shaped slot is etched from the graphene patch. SiO₂ substrate, having permittivity 3.9, is used to design the proposed antenna. The ground plane along with the microstrip line is made up of a conductor. Gold and silver are two choices for the same. The use of gold gives better performance because of its better conductivity as well as lower oxidation rate. However, it is very costly. Therefore, silver can be used. It cannot oxidize rapidly. The optimized antenna dimension is given in the caption of Fig. 1. Drude's model is used to obtain the dispersive features of silver. It is mathematically given by the following formula [5]:

$$\epsilon_{\text{silver}} = \epsilon_{\text{air}} \left[\epsilon_{\infty} - \frac{f_p^2}{\{f + if_{cl}\}} \right] \quad (1)$$

In Eq. (1), 'ε' shows the permittivity; 'ε_∞' real part of the dielectric constant, f_p and f_{cl} is the plasma frequency and collision frequency respectively. The value of ε_∞, f_p and f_{cl} is taken as 5, 2175 THz, and 4.35 THz respectively [5]. The dispersive feature of exciting structure can be selected in such a way that transmission losses are minimum at THz frequency.

iii. Antenna Analysis

In this section, step by step analysis of the proposed circularly polarized THz antenna is described. At the THz frequency range, spatial distribution in the graphene-based patch is expected to be absent [10]. Now, with the assistance of Kubo's formula, the thickness of the graphene layer i.e. 0.34 nm is placed over the SiO₂-based substrate. In the THz frequency range, the energy of a photon is negligible as compared to Fermi energy [11]. Therefore, the value of interband conductivity of graphene is quite low as compared to intraband conductivity. Its intraband conductivity can be mathematically given as follows [12]:

$$\sigma_{\text{intraband}}(\omega, \mu_c, \Gamma, T) = -j \frac{e^2 k_B T}{\pi h^2 (\omega - j2\Gamma)} \left(\frac{\mu_c}{k_B T} + 2 \ln \left(e^{\frac{\mu_c}{k_B T}} + 1 \right) \right)$$

2

In CST-MWS simulation software, graphene material is placed with relaxation time $\tau = 1$ ps, temperature $T = 300$ k [13]. Figure 2 shows the variation of intraband conductivity of graphene with different values of chemical potential. The main observation obtained from Fig. 2 is that the conductivity of graphene alters with variation in chemical potential. This indicates the tunable feature can be achieved in a graphene-based patch with the alteration of chemical potential. Figure 3 displays the variation in |S₁₁| with and without a tilted dumbbell-shaped slot. From Fig. 3, it can be observed that the loading of the slot over the graphene patch shifts the resonance peak to a higher frequency range. It is due to a reduction in the effective permittivity of the radiator [14]. The proposed dumbbell-shaped aperture is the diagonally

perturbed circular-shaped aperture. Figure 4 shows $|S_{11}|$ optimization of the radius of the circular-shaped aperture. From Fig. 4, it can be observed that as the radius of the slot increases, resonant frequency shifts in a forward direction. It is due to a reduction in effective permittivity. On the other hand, impedance matching degrades with radius increases. The optimum value of R is taken as 2.0 μm .

Figure 5 displays the axial ratio variation with and without a tilted dumbbell-shaped slot. It is perceived from Fig. 5 that CP waves are obtained with the loading of the proposed slot within the desired frequency band i.e. 5.85 THz to 5.95 THz. To produce the CP feature in any radiator, two conditions must be fulfilled: (i) creation of degenerated orthogonal modes; and (ii) 90° phase shift between the modes [4]. For satisfying this condition in the proposed radiator, a circular aperture is loaded first. It can create two orthogonal degenerated modes with the same amplitude. After that, the circular aperture is perturbed diagonally. The degree of perturbation creates the path delay between the orthogonal components, which in turn creates the desired phase difference i.e. 90° . Figure 6 shows the optimization of a degree of perturbation of the circular aperture. From Fig. 6, it can be observed that the optimum value of AR is obtained, when the circular aperture is perturbed diagonally with an angle of 45° . In other words, it can be said that the dumbbell-shaped slot is tilted at an angle of 45° .

Figure 7 displays the magnitude of E-field variation on graphene patch with and without slot at 5.9 THz. From Fig. 7, it can be observed that the variation of the E-field is uniform about the X-axis in the absence of a slot, while it is distorted after loading the dumbbell-shaped slot. It is allied diagonally. This phenomenon indicates the creation of CP waves. TM_{41} mode is supported by the proposed graphene-shaped aperture [7].

Another important significance of the graphene patch is its capability of tuning by simply varying the chemical potential. Figure 8 and Fig. 9 show the reflection coefficient and axial ratio variation with change in chemical potential (u_c). As the value of chemical potential increases, resonance frequency shifts towards the higher frequency band. AR values also change in the same way. Change in chemical potential does not create many effects on orthogonal mode formation. However, some small changes may occur in the amplitude of the modes, which will create a small effect on the value of AR.

Easy controlling of the sense of circular polarization is also an important feature of the proposed antenna. Figure 10 displays the LHCP and RHCP pattern in the XZ plane at 5.9 THz with a proposed aperture as well as a mirror image of the proposed aperture. From Fig. 10, it is clearly observed that the antenna is left-handed circularly polarized (LHCP) with the proposed aperture, while it is right-handed circularly polarized with a mirror image of the proposed aperture. That means, a change in orientation simply changes the orientation of the field.

Iv. Optimized Outcomes Of Proposed Radiator

In this section, the optimized outcome of the proposed radiator is discussed and compared with the HFSS EM simulator. Figure 11 displays the $|S_{11}|$ variation of the proposed antenna with CST-MWS and HFSS

EM simulator. There is good agreement between the $|S_{11}|$ variations obtained from both the software. From Fig. 11, it is confirmed that the proposed antenna works from 5.85 THz to 6.05 THz.

Figure 12 displays the axial ratio variation with HFSS and CST-MWS software. From Fig. 12, it is confirmed that the proposed antenna supports the CP waves from 5.85 THz to 5.95 THz. There is good agreement between the results obtained from HFSS and CST-MWS. Figure 13 shows the gain variation of the proposed antenna. From Fig. 13, it is perceived the gain value is around 5.5 dBi in the operating frequency band. Figure 14 displays the 2D LHCP and RHCP radiation pattern in XZ and YZ planes at 5.9 THz. From Fig. 14, it is concluded that the proposed antenna acts as a left-handed circularly polarized antenna.

V. Conclusion

In this article, a tunable graphene-based radiator is designed and analyzed at THz frequency. Loading of tilted dumbbell-shaped patch incorporates the circular polarization feature in the proposed antenna. The proposed antenna works from 5.85 THz to 6.05 THz with supporting TM_{41} mode. The proposed antenna shows a good gain value i.e. 5.5 dBi along with broadside radiation characteristics. A feature of CP waves at THz frequency makes the proposed radiator suitable for biomedical applications.

Declarations

***Ethics approval and consent to participate:** Not Applicable

*** Consent for publication:** I, Ajay Kumar Dwivedi, give my consent for the publication of identifiable details, which can include photograph(s) and/or videos and/or figures and/or details within the text ("Material") to be published in the above Journal and Article

*** Availability of data and materials:** Not Applicable

*** Funding:** No funds, grants, or other support was received.

*** Authors' contributions:** Conceptualization and Methodology [Nagesh Kallollu Narayaswamy]; Writing - revised draft preparation: [Krishna Kanth Varma Penmatsa]; Analysis and Investigation: [Manju Ramrao Bhosle]; Writing - original draft preparation and Supervision: [Ajay Kumar Dwivedi]

*** Disclosure of potential conflicts of interest:** There are no potential conflicts of interest.

*** Research involving Human Participants and/or Animals:** Not Applicable

*** Acknowledgements:** Not Applicable

ORCID ID

Ajay Kumar Dwivedi <http://orcid.org/0000-0003-1146-0902>

References

1. Federici, J., Moeller, L.: Review of terahertz and subterahertz wireless communications. *J. Appl. Phys.* **107**, 111101 (2010). <https://doi.org/10.1063/1.3386413>
2. Akyildiz, I.F., Jornet, J.M., Han, C.: Terahertz band: next frontier for wireless communications. *Phys. Commun.* **12**, 16–32 (2014)
3. Ariza, M.P., Ortiz, M.: Discrete dislocations in graphene. *J. Mech. Phys. Solids.* **58**, 710–734 (2010). <https://doi.org/10.1016/j.jmps.2010.02.008>
4. Balanis, C.A.: *Antenna Theory: Analysis and Design*, 3rd edn. A John Wiley & Sons, New York, USA (2005)
5. Gaurav Varshney, S., Gotra, J., Kaur, V.S., Pandey, Yaduvanshi, R.S.: Obtaining the circular polarization in a nanodielectric resonator antenna for photonics applications. *Semicond. Sci. Technol.* **34**, 1–9 (2019)
6. Shahid Ullah, C., Ruan, M.S., Sadiq, T., He, W.: “Microstrip system on-chip circular polarized (CP) slotted antenna for THz communication application”, *Journal of Electromagnetic Waves and Applications*, **34**, 1029–1038 (2020)
7. Gaurav Varshney, S., Debnath, Sharma, A.K.: “Tunable circularly polarized graphene antenna for THz applications” *Optik-International Journal of Light and electron optics*, **223**, 220,1–10
8. Shalini, M., Ganesh Madhan, M.: A compact antenna structure for circular polarized terahertz radiation. *Optik-International J. Light electron Opt.* **231**, 1–11 (2021)
9. Gupta, R., Varshney, G., Yaduvanshi, R.S.: Tunable terahertz circularly polarized dielectric resonator antenna. *Optik-International J. Light electron Opt.* **239**, 1–7 (2021)
10. Cabellos-Aparicio, A., Llatser, I., Alarcón, E., Hsu, A., Palacios, T.: Use of terahertz photoconductive sources to characterize tunable graphene RF plasmonic antennas. *IEEE Trans. Nanotechnol.* **14**, 390–396 (2015)
11. Varshney, G., Verma, A., Pandey, V.S., Yaduvanshi, R.S., Bala, R.: A proximity coupled wideband graphene antenna with the generation of higher order TM modes for THz applications. *Opt. Mater. (Amst)*. **85**, 456–463 (2018)
12. Falkovsky, L.A., Pershoguba, S.S.: Optical far-infrared properties of a graphene monolayer and multilayer. *Phys. Rev. B–Condens Matter Mater. Phys.* **76**, 1–4 (2007)
13. Mohammadreza Razavizadeh, S.: Simulation of Graphene in CST Microwave v2015 and COMSOL Multiphysics, 5.2a, (2017)
14. Bharti, G., Kumar, D., Gautam, A.K., Sharma, A.: Two-port dual-band circularly polarized dielectric resonator-based MIMO antenna with polarization diversity. *Electromagnetics.* **40**, 463–478 (2020)

Figures

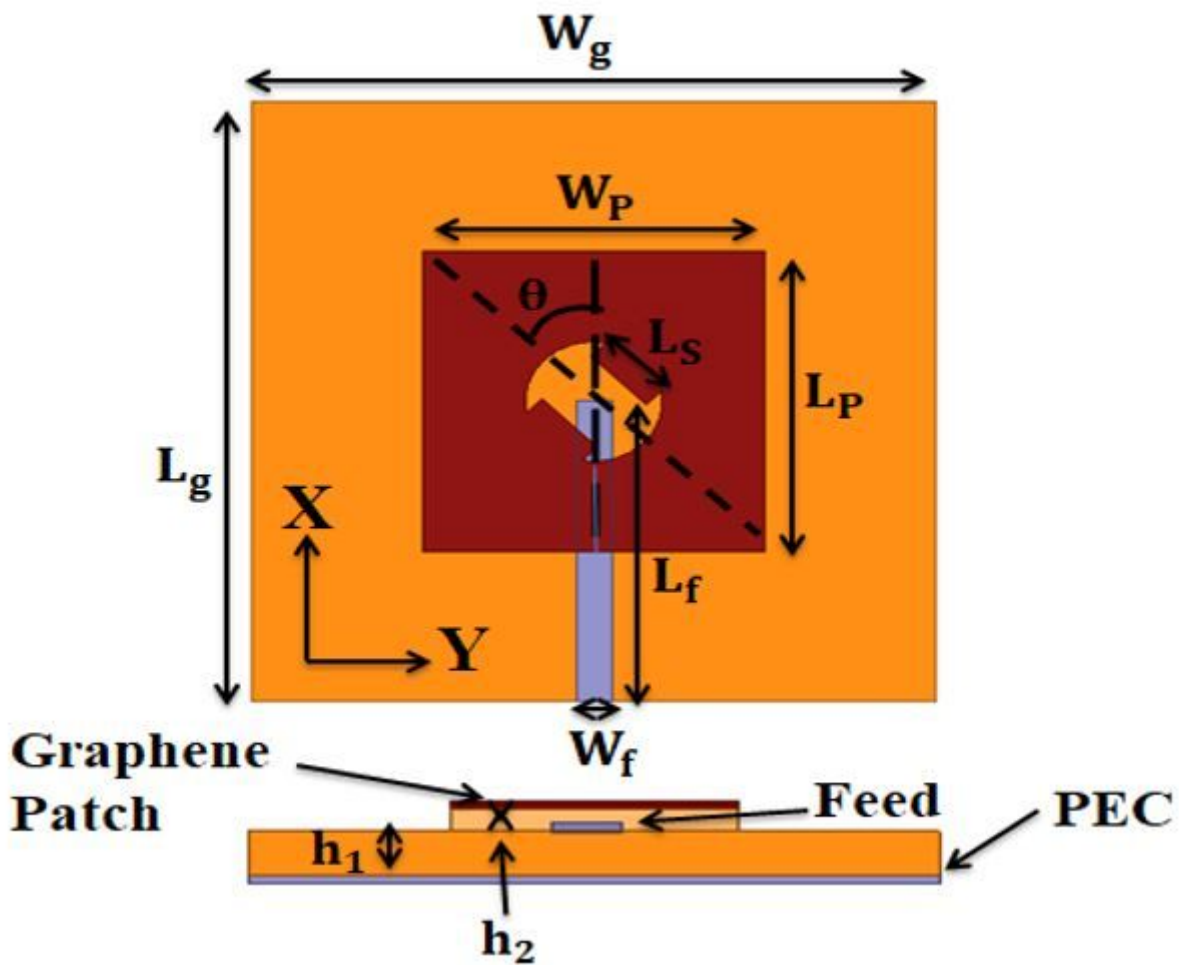


Figure 1

Structural Layout of proposed THz antenna with Top and side view; $W_g = 60\mu\text{m}$; $L_g=60\mu\text{m}$; $L_p=24\mu\text{m}$; $W_p = 36\mu\text{m}$; $L_f= 39\mu\text{m}$; $W_f= 1.8\mu\text{m}$; $L_s=$; $h_1 = 0.8\mu\text{m}$; $h_2 = 0.4\mu\text{m}$

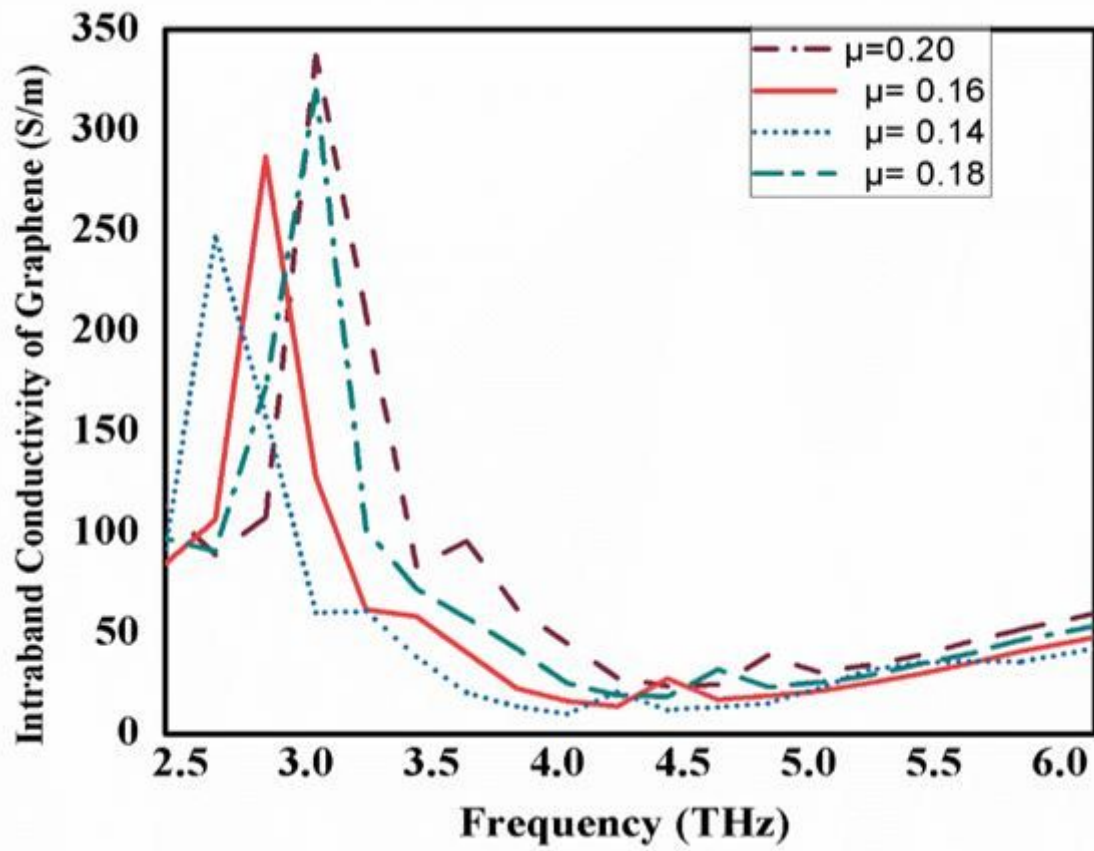


Figure 2

Variation of Intradband Conductivity of Graphene with alteration in chemical potential

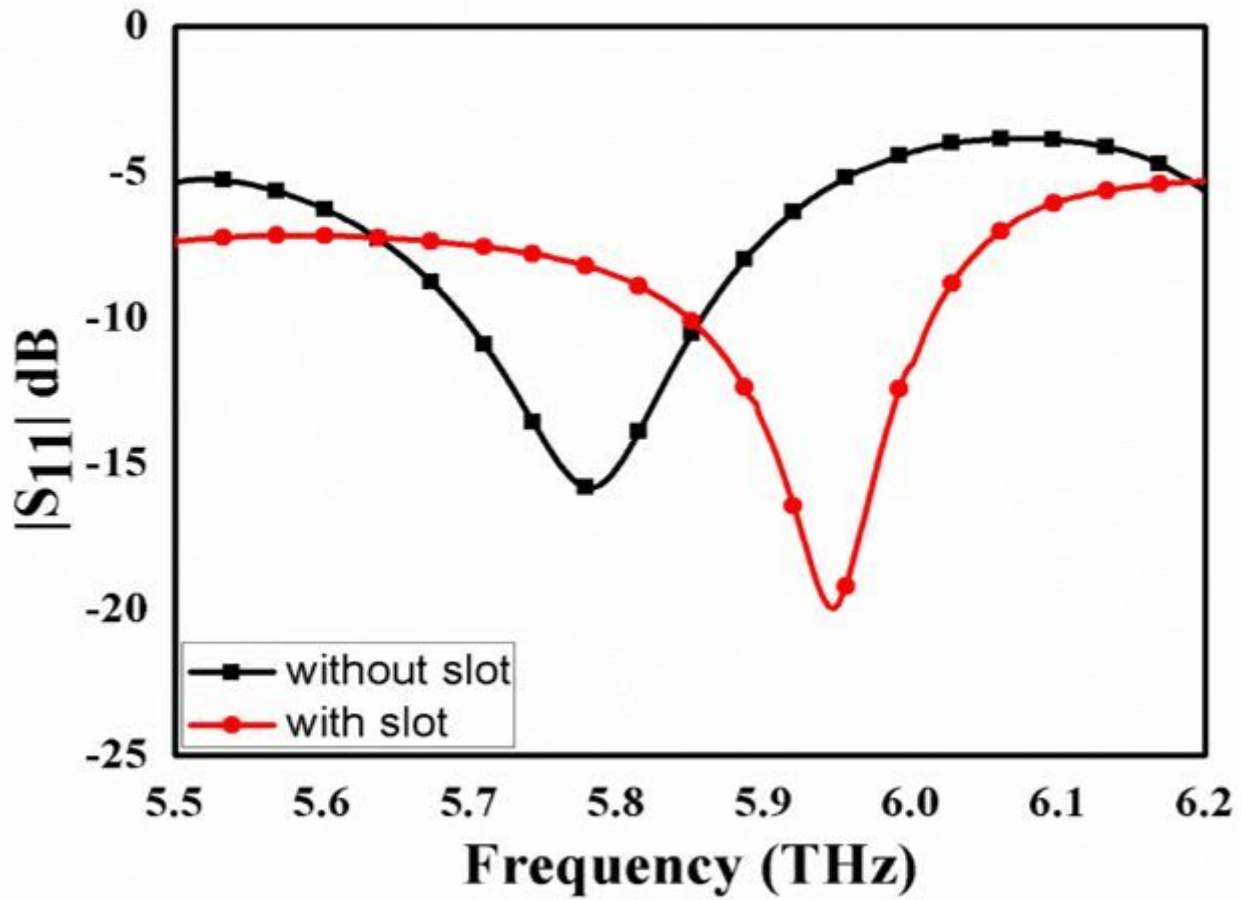


Figure 3

Reflection Coefficient variation with and without tilted dumbbell slot

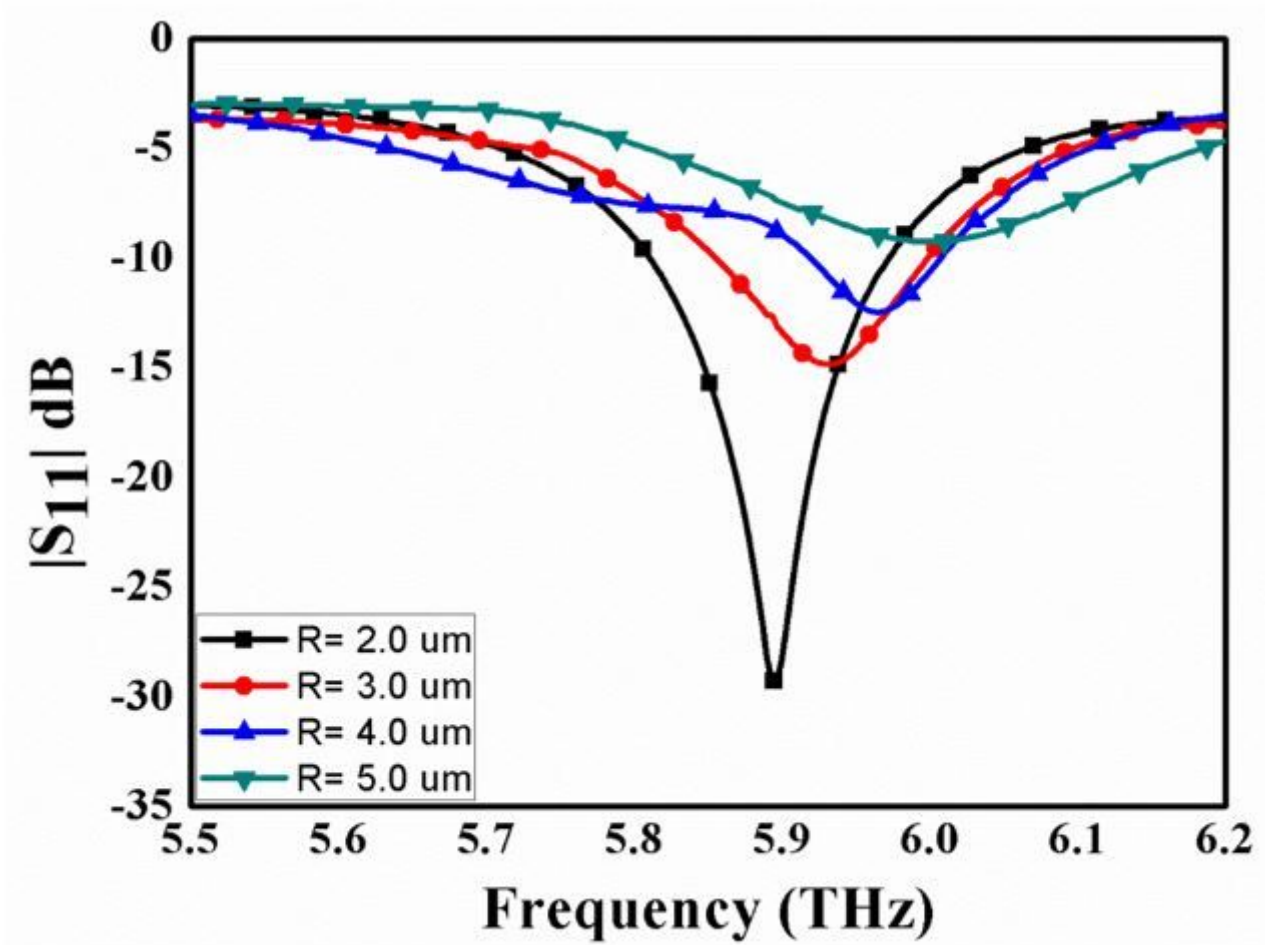


Figure 4

Reflection Coefficient variation with change in radius of aperture (R)

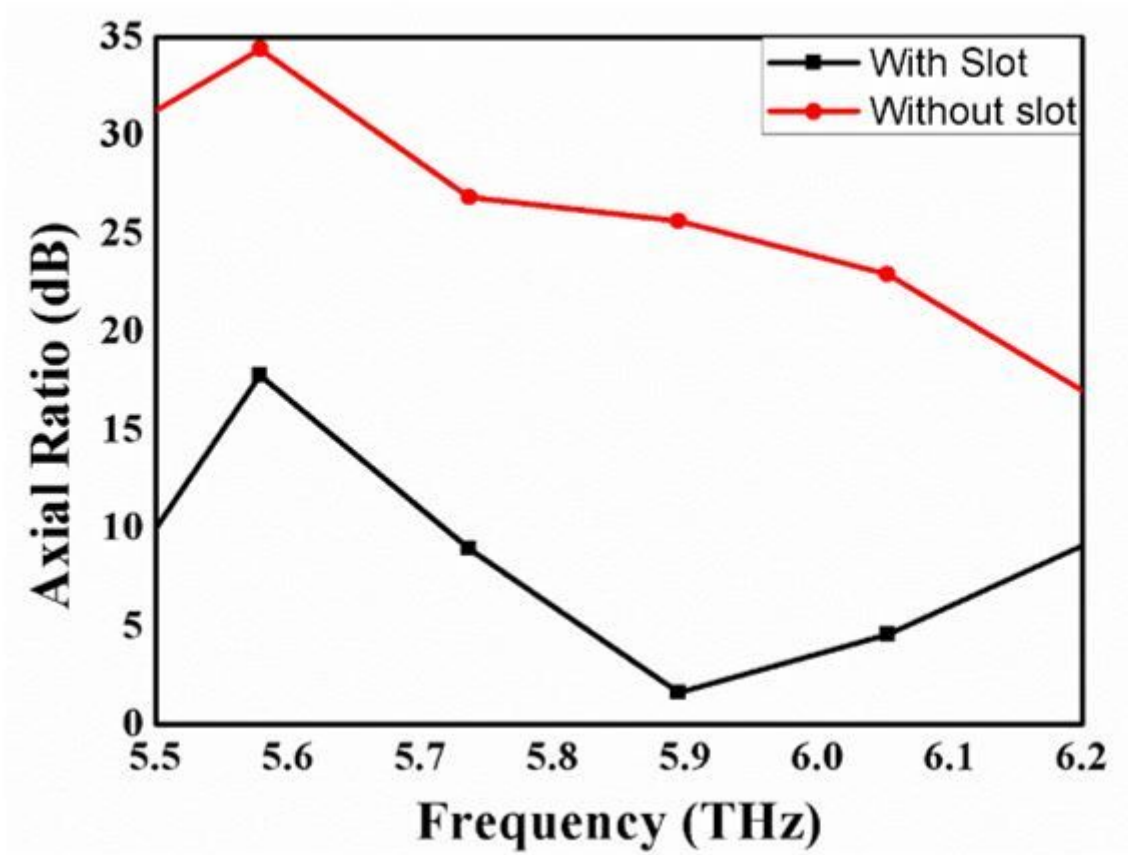


Figure 5

Axial Ratio variation with and without slot loading

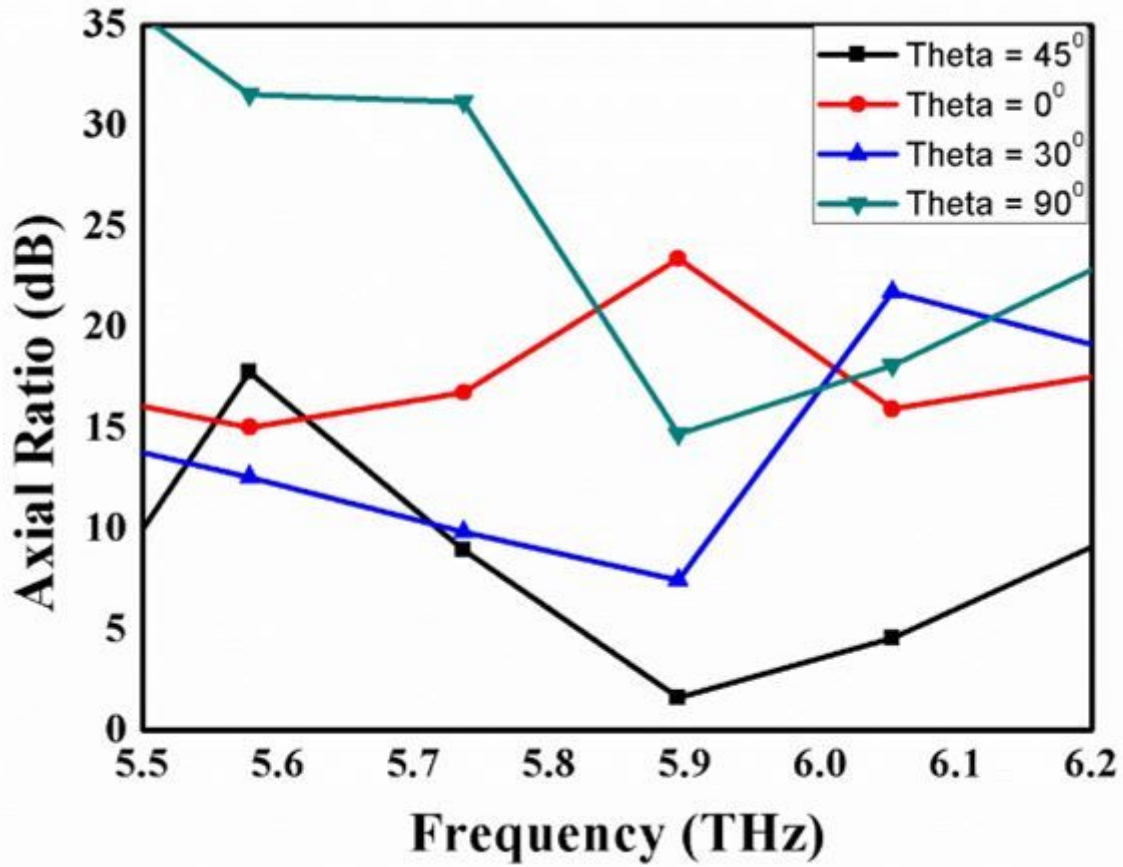


Figure 6

Axial Ratio variation with different tilting of dumbbell-shaped aperture

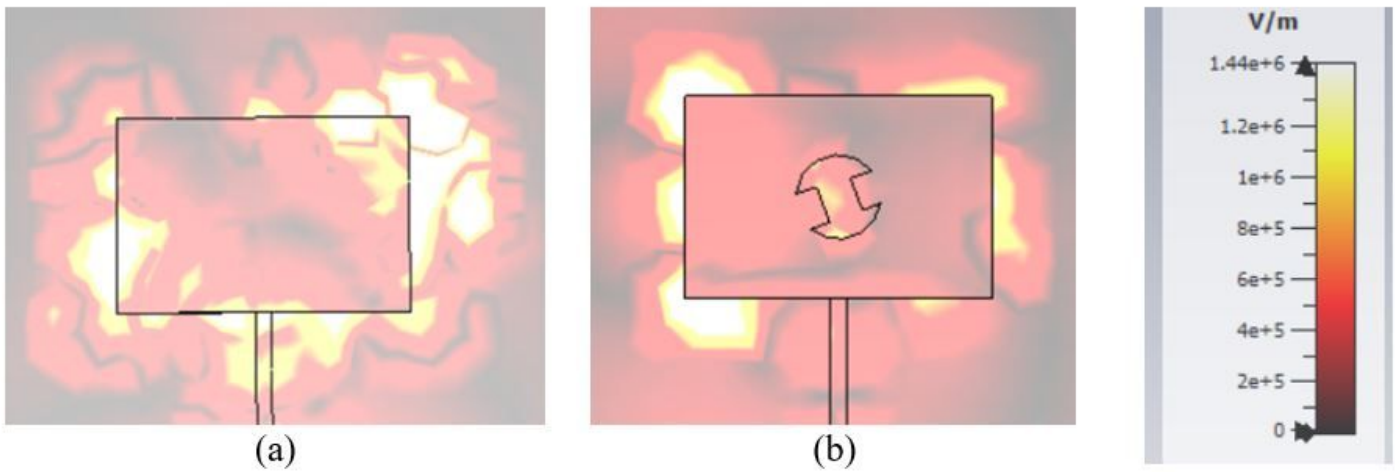


Figure 7

Magnitude of E-field over graphene patch at 5.9 THz (a) without slot (b) with slot

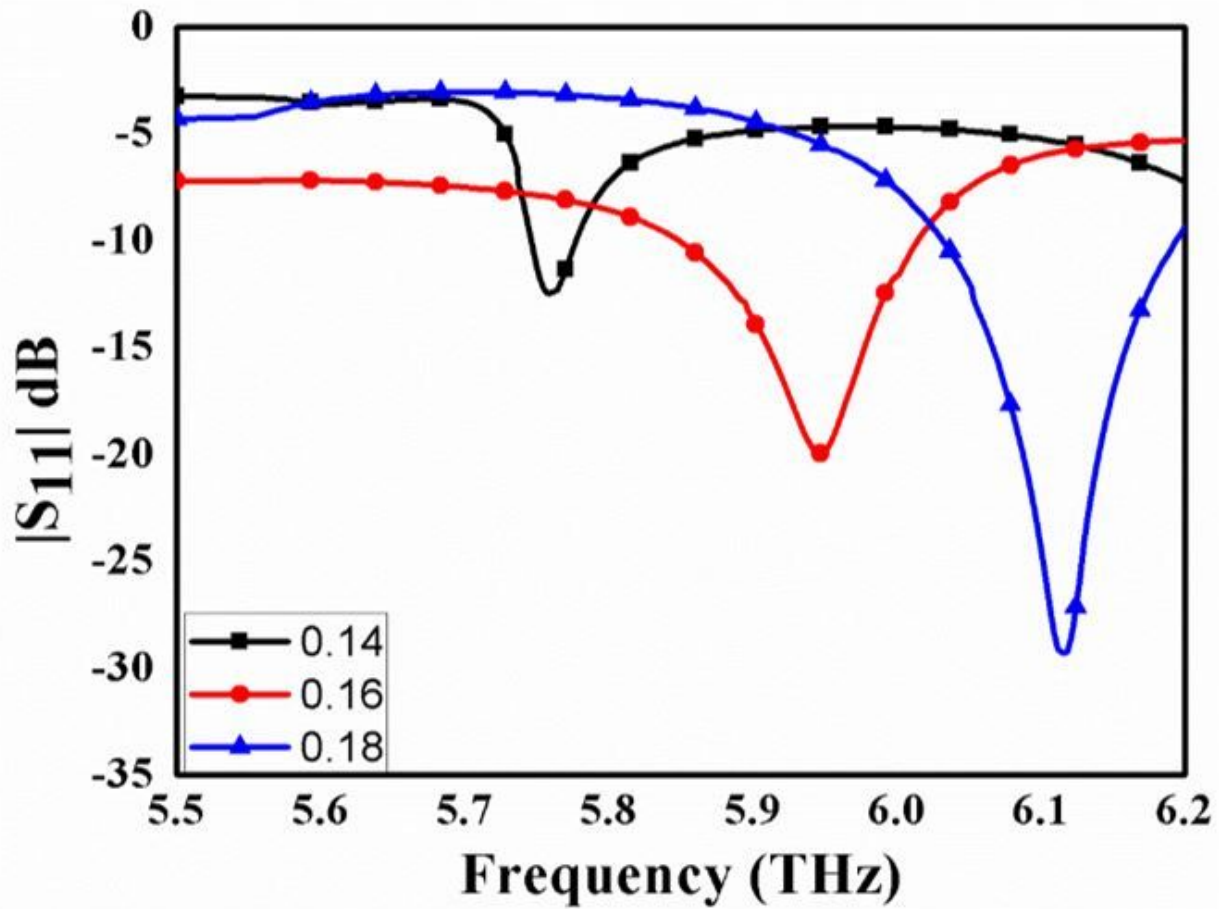


Figure 8

$|S_{11}|$ variation with change in chemical potential (u_C)

Figure 9

Axial Ratio variation with change in chemical potential (u_C)

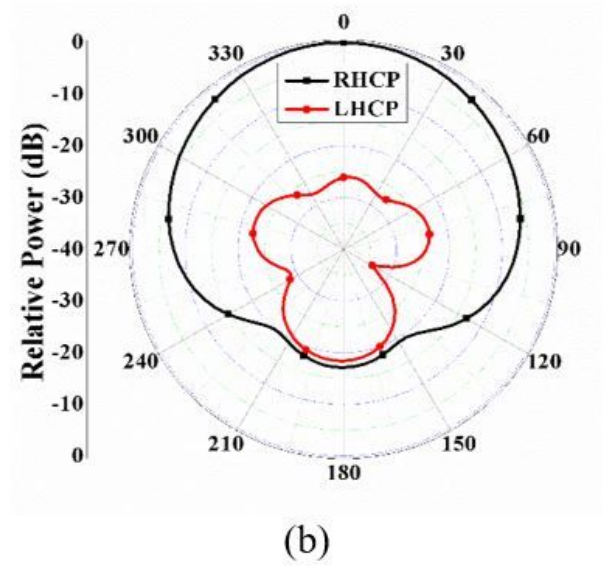
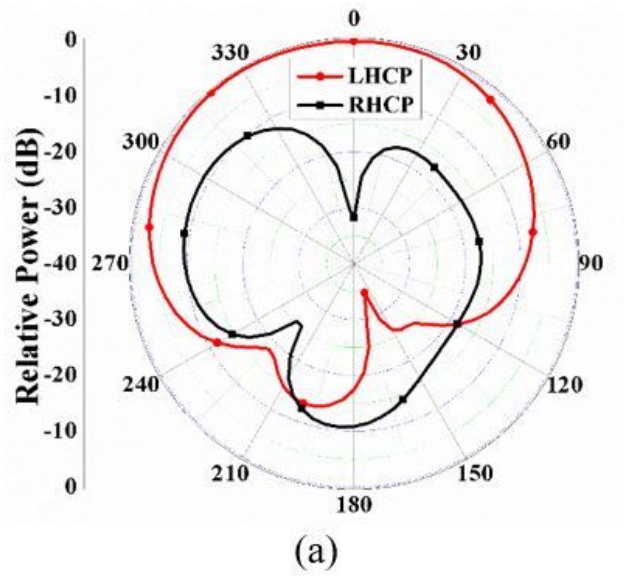


Figure 10

Radiation Pattern of Proposed Antenna at 5.9 THz (a) proposed aperture (b) mirror image of the proposed aperture

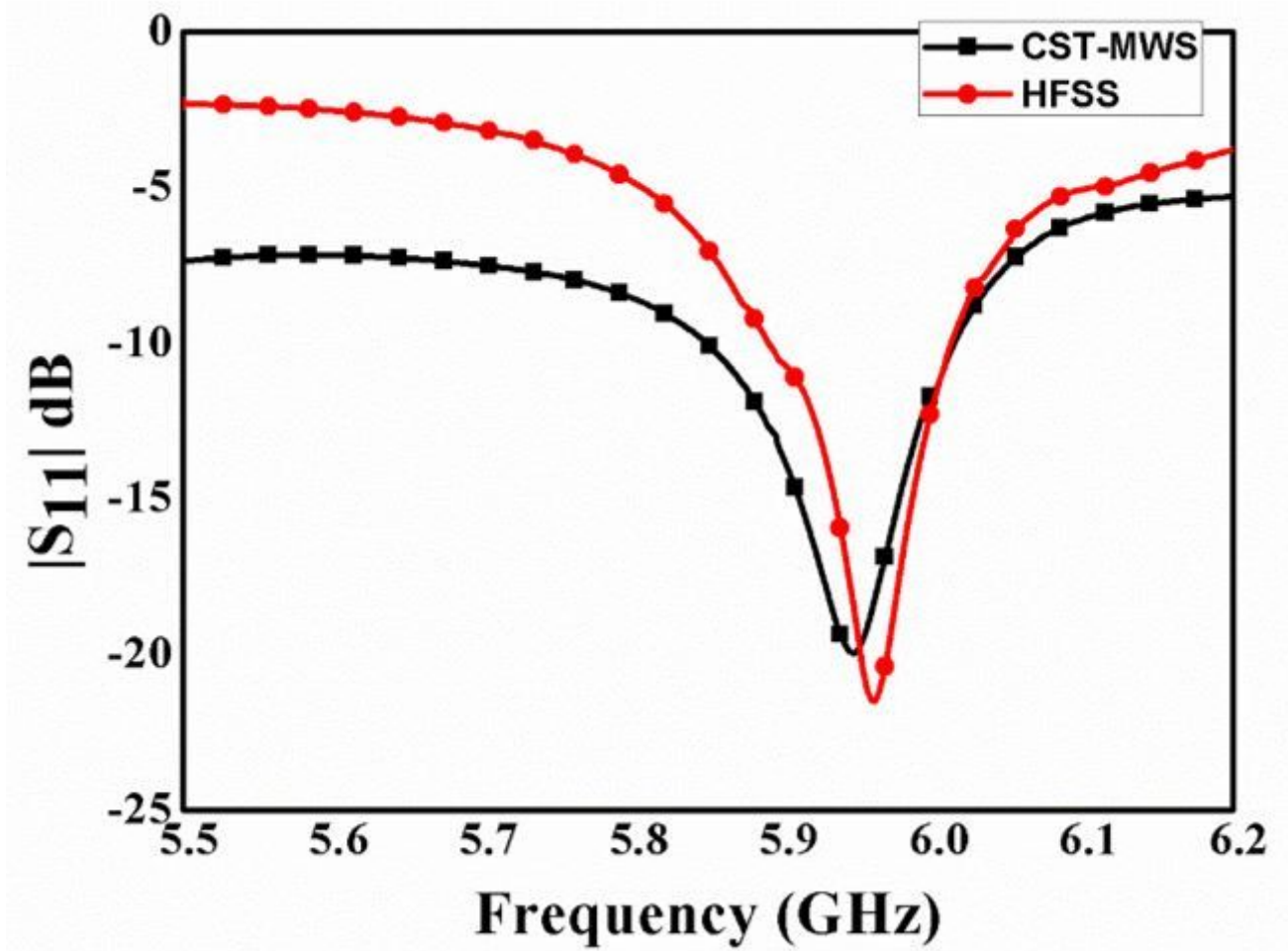


Figure 11

Optimized $|S_{11}|$ variation of the proposed antenna

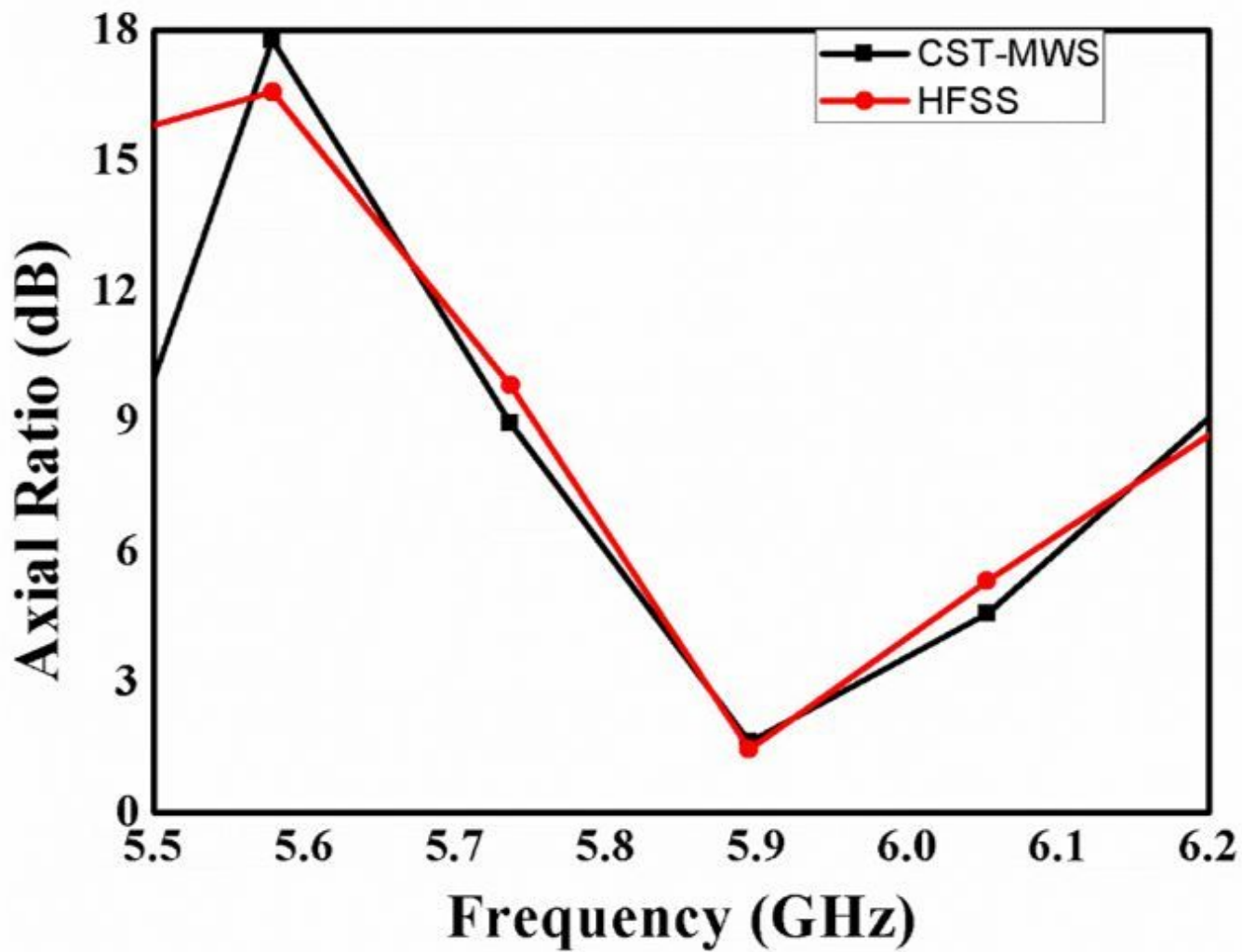


Figure 12

Optimized Axial ratio variation of proposed antenna

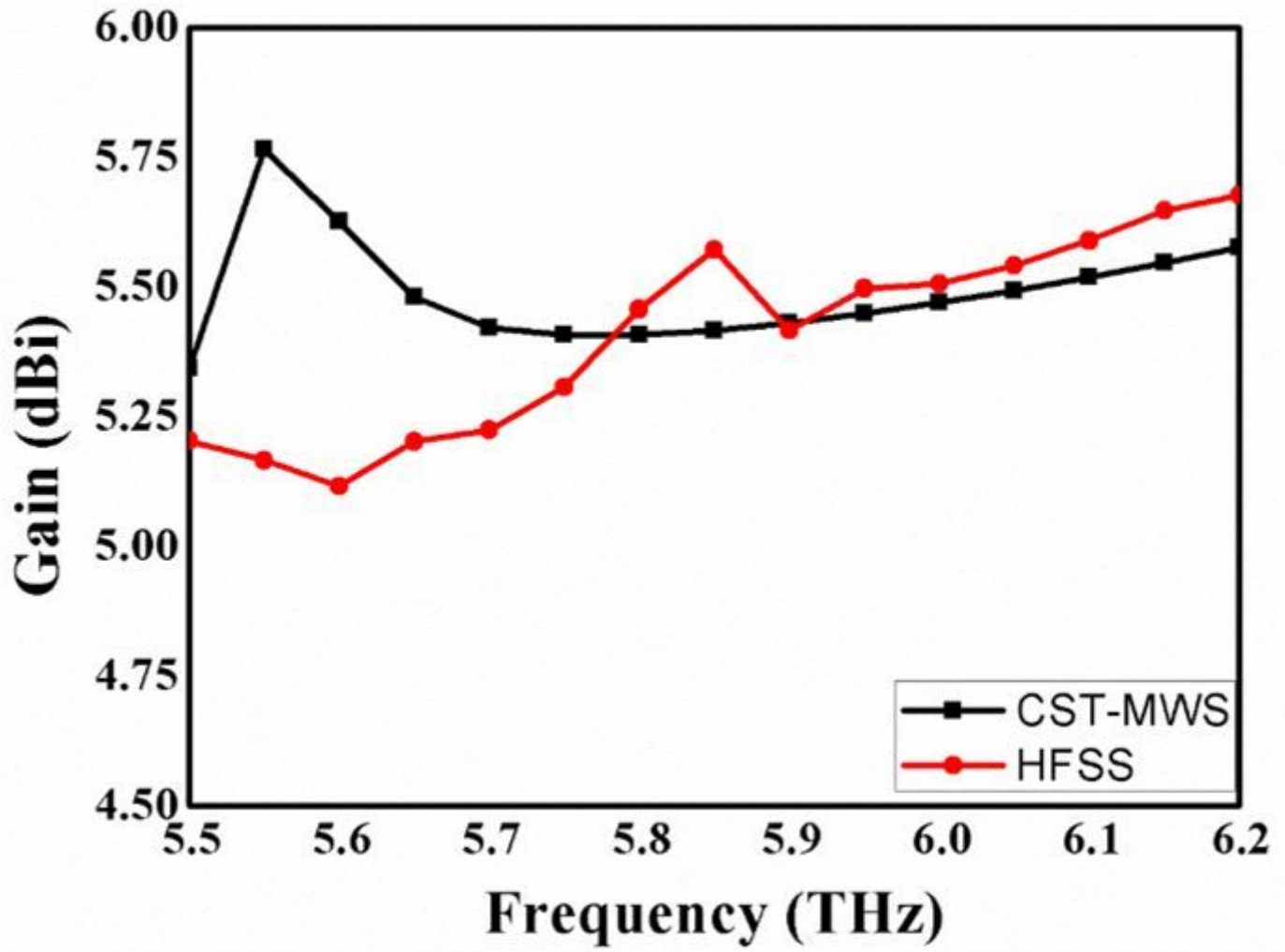


Figure 13

Gain variation of the proposed antenna with frequency

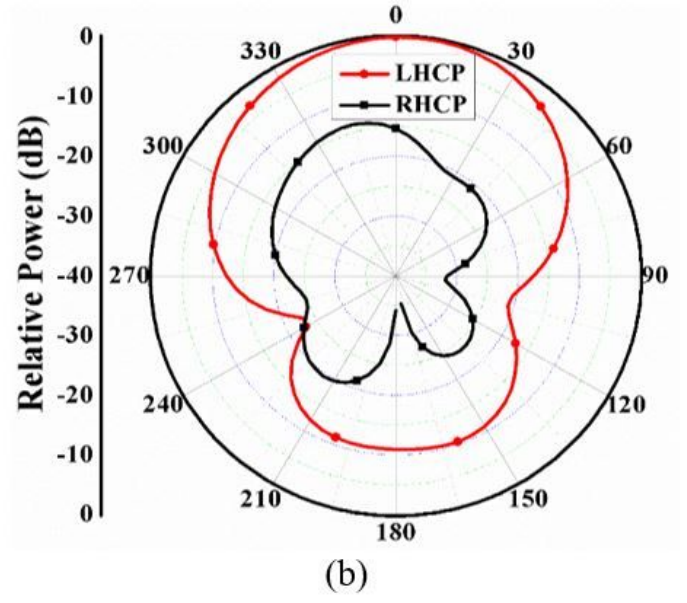
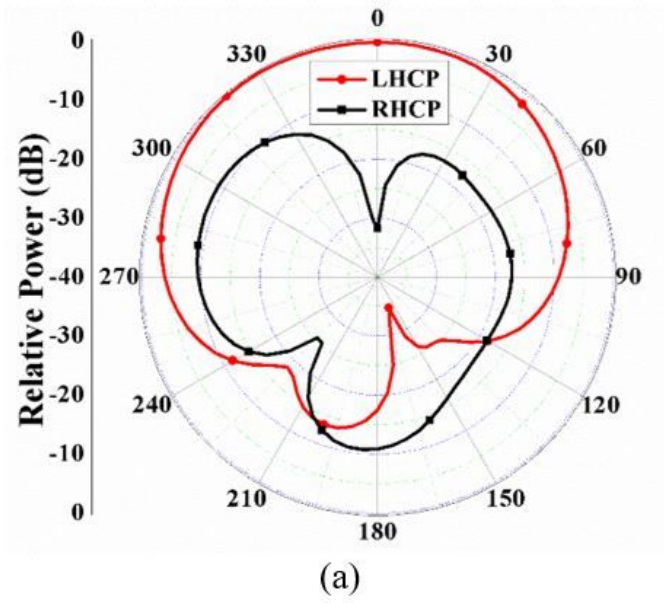


Figure 14

Radiation pattern of proposed antenna at 5.9 THz (a) XZ plane (b) YZ plane